



Isoenzyme- and Allozyme-Specific Inhibitors: 2,2'-Dihydroxybenzophenones and Their Carbonyl N-Analogues that Discriminate between Human Glutathione Transferase A1-1 and P1-1 Allozymes

Foteini M. Poulou¹, Trias N. Thireou²,
Elias E. Eliopoulos², Petros G. Tsoungas³,
Nikolaos E. Labrou¹ and Yannis D. Clonis^{1,*}

¹Laboratory of Enzyme Technology, Department of Biotechnology, Agricultural University of Athens, Athens, Greece

²Laboratory of Genetics, Department of Biotechnology, Agricultural University of Athens, Athens, Greece

³Laboratory of Biochemistry, Hellenic Pasteur Institute, Athens, Greece

*Corresponding author: Yannis D. Clonis, clonis@aua.gr

The selectivity of certain benzophenones and their carbonyl N-analogues was investigated towards the human GSTP1-1 allozymes A, B and C involved in MDR. The allozymes were purified from extracts derived from *E. coli* harbouring the plasmids pEXP5-CT/TOPO-TA-hGSTP1*A, pOXO4-hGSTP1*B or pOXO4-hGSTP1*C. Compound screening with each allozyme activity indicated three compounds with appreciable inhibitory potencies, 12 and 13 with P1-1A 62% and 67%, 11 and 12 with P1-1C 51% and 70%, whereas that of 15 fell behind with P1-1B (41%). These findings were confirmed by IC₅₀ values (74–125 μM). Enzyme inhibition kinetics, aided by molecular modelling and docking, revealed that there is competition with the substrate CDNB for the same binding site on the allozyme ($K_{i(13/A)} = 63.6 \pm 3.0 \mu\text{M}$, $K_{i(15/B)} = 198.6 \pm 14.3 \mu\text{M}$, and $K_{i(11/C)} = 16.5 \pm 2.7 \mu\text{M}$). These data were brought into context by an *in silico* structural comparative analysis of the targeted proteins. Although the screened compounds showed moderate inhibitory potency against hGSTP1-1, remarkably, some of them demonstrated absolute isoenzyme and/or allozyme selectivity.

Key words: allozyme, benzophenone, enzyme cloning, enzyme inhibition, enzyme kinetics, human glutathione transferase, isoenzyme, ketoxime, N-acyl hydrazone, protein structure comparative analysis

Received 19 January 2015, revised 1 April 2015 and accepted for publication 3 April 2015

Benzophenones, along with bioflavonoids, coumarins and xanthenes, constitute a major class of compounds exhibiting multiple biological activities (1). *o*-Hydroxybenzophenone derivatives, in particular, are ubiquitous in nature but also synthetically obtained compounds, for example certain combretastatins and phenstatins (2). Our recently reported interest in utilizing the reactivity profile of xanthone (3) in synthesis (4,5), as well as its inhibitory potential towards the medically important human isoenzyme glutathione transferase A1-1 (hGSTA1-1) (6), prompted us to investigate xanthone ring-opened analogues, substituted 2,2'-*o*-dihydroxybenzophenones, towards hGSTA1-1 (7), taking advantage of their structure similarities, in pursuit of promising inhibitor lead structures against this enzyme, involved in multiple drug resistance (MDR). To that end, GSTs (EC 2.5.1.18) are cell-detoxifying agents, for they catalyse the coupling of glutathione (GSH) to hydrophobic xenobiotic and endogenous compounds, rendering them hydrophilic and, thus, facilitating their metabolic processing and eventual secretion from the cell (8). Based on the same detoxification mechanisms, cancer cells often acquire resistance by overexpressing GSTs (9), hampering the effectiveness of certain chemotherapeutic drugs. In particular, GSTs of the π class are the most studied isoenzymes in human cancer. Their expression levels vary with tumour type and stage, hence affecting the effectiveness of anticancer drugs, for example thiotepa and chlorambucil (10–12). Therefore, certain GST-recognizing drugs and prodrugs have been suggested to overcome MDR attributed to GST overexpression (13–15). For example, the prodrug TLK286 (Telcyta) is activated by hGSTP1-1, after being triggered by Tyr7 located in the active region of the isoenzyme (16). As tumour-protective phenomena may vary by patient GST isoenzyme/allozyme profiles, we thought to study dihydroxybenzophenones and their carbonyl N-analogues as inhibitors discriminating not only between A1-1 and P1-1 hGST isoenzymes but also between hGSTP1-1 allozymes A, B and C, involved in MDR (17).

Materials and Methods

Expression and purification of hGSTP1-1 allozymes

The expression was based on a published method with modifications (18), whereas the enzyme purification procedures were developed in our laboratory (Appendix S1).

Routine enzyme assay for determining GST activity

Determination of GST activity was performed by monitoring the formation of the conjugate between CDNB and GSH at 340 nm ($\epsilon = 9600$ L/mole/cm) at 6.5 and 25 °C. One unit of enzyme activity is defined as the amount of enzyme that produces 1.0 μ mole of product per minute under the assay conditions (7).

Compound screening as inhibitors for hGSTP1-1 allozymes ('cherry picking')

'Cherry picking' was performed by introducing the ingredients in the following order (1 mL final assay volume): potassium phosphate buffer (approx. 100 mM final, pH 6.5), CDNB (20 μ L from 50 mM stock solution prepared in ethanol; 1.0 mM final), test compound (20 μ L from 5 mM stock solution in DMSO; 0.1 mM final) and enzyme (typically, 80 μ L from hGSTP1A producing 0.0370 ΔA_{340} /min, 50 μ L from hGSTP1B producing 0.0491 ΔA_{340} /min and 35 μ L from hGSTP1C (previously diluted with buffer, 1:10 v/v) producing 0.0502 ΔA_{340} /min). After mixing, the reaction started by adding GSH (20 μ L from 125 mM stock prepared in water; 2.5 mM final) and continued for 1 min at 25 °C. The observed rate was used to calculate the remaining activity (%), taking as 100% initial activity value the rate observed, after replacing the test compound by an equal volume of DMSO which, in all assays, was maintained at a 2% v/v final concentration.

Determination of IC_{50} values for inhibitors selected from 'cherry picking'

Initial velocities for the GST-catalysed reaction with CDNB (1 mM) and GSH (2.5 mM) as substrates were measured at 25 °C, in the presence of various concentrations of the inhibitors selected from 'cherry picking', using the same assay conditions (see previous paragraph). Different inhibitor quantities, in 20 μ L DMSO, were introduced in the assay mixture. The observed rate was used to calculate the remaining activity (%), taking as 100% initial activity value the observed rate, after replacing the inhibitor by an equal volume of DMSO (20 μ L). The IC_{50} values were determined from a graph depicting remaining GST activity (%) against inhibitor concentration.

Kinetic analysis of inhibitors selected from 'cherry picking'

Initial velocities for the GST-catalysed reaction with CDNB as variable substrate were determined in reaction mixtures of a total volume of 1 mL (25 °C) containing potassium phosphate buffer (100 mM, pH 6.5), 2.5 mM GSH and different concentrations of CDNB (60–2100 μ M with hGSTP1A, 75–2100 μ M with hGSTP1B and 37.5–2100 μ M with hGSTP1C) in the absence and presence of inhibitor **13** (0, 25 and 50 μ M with hGSTP1A) or inhibitor **15** (0, 40, 80 and 100 μ M with hGSTP1B) or inhibitor **11** (0, 15, 30, 70 and 100 μ M with hGSTP1C). Initial velocities for the hGSTA1-1-catalysed reaction with GSH as variable substrate were determined in reaction mixtures of a total volume of 1 mL (25 °C) containing potassium phosphate buffer (100 mM, pH 6.5), 1 mM CDNB and different concentrations of GSH (45–2500 μ M) in the absence and presence of inhibitor **11** (0, 15, 30 and 60 μ M).

Modelling and docking: the in silico structures of hGSTPs and docking of the 2,2'-dihydroxybenzophenones and their carbonyl N-analogues

The structure of hGSTP1-1 (variant or allozyme A) in complex with ethacrynic acid and its glutathione conjugate was downloaded from the Protein Data Bank (PDB code 11GS) and prepared with the Protein Preparation Wizard (19) in Maestro (Schrodinger, LLC, New York, NY, USA). Two further variants (allozymes B and C), according to their amino acid substitutions in positions 104 and 113, were constructed, using the X-ray structure of allozyme B (PDB code 1PGT) and a constructed model for the mutant of the external surface mutation Ala113Val, defining the optimal rotamers of the respected side chains using 12 nseconds molecular dynamics on DESMOND 3.6 (20). Rotamers were displayed with PyMOL (Figure S1). A docking grid, including the tripeptide substrate glutathione, was set up centred on ethacrynic acid (Table S1). OMEGA 2.5.1.4 (OpenEye Scientific Software) (21) was used to generate molecular conformations of the synthetic analogues. Potentially active compounds with a similar shape to parental compounds were identified by ROCS 3.2.0.4 (22) fast shape comparison application. The synthetic analogues were docked flexibly using Glide SP (23,24) (Table S1). Docking results (Table S2a,b,c) were both visually inspected and quantitatively evaluated based on a docking score. Docking results were checked for positional stability using postdocking molecular dynamics with Desmond 3.6 (Table S3). All figures depicting 3D models were created using PYMOL, version 1.7.4 (Schrodinger, LLC).

Results and Discussion

The hGSTP1 allozymes were purified on a GSH-affinity chromatography column (enzyme desorption with 10 mM GSH),

leading to enzyme preparations of good purification characteristics and overall protocol performance (Table S4).

Compound screening and selection of inhibitors for hGSTP1-1

To reveal the enzyme inhibitory potency of the 2,2'-dihydroxybenzophenones and their carbonyl N-analogues, all compounds were subjected to screening against the three allozymes, hGSTP1A, hGSTP1B and hGSTP1C. In designing the screening enzyme assay protocol against hGSTP1-1, the concentration of 100 μM was chosen. This choice was dictated by preliminary experiments run at concentrations in the range 1–30 μM , as suggested in the literature (7,25), showing the compounds not to be as effective inhibitors with the P1-1 isoenzyme as they were with A1-1 (7). A more crucial factor to be decided has been the substrate concentration, CDNB, in the enzyme inhibition assay for 'cherry picking' and IC_{50} determinations. Having initially considered the known Michaelis constant for the CDNB-hGSTP1-1 couple ($K_m = 0.98 \pm 0.06 \text{ mM}$) (17), we performed inhibition assays at $[\text{CDNB}] = 1 \text{ mM}$, fulfilling the so-called balanced assay conditions, that is $[\text{CDNB}] \approx K_m$, acknowledged in the literature as the optimum choice (6,7,25). From the screening data obtained (Table 1, Figure S2), one distinguishes three groups of inhibitory potency against the hGSTP1 allozymes (Table S5): <20% (low inhibition), 20–40% (medium inhibition) and 50–80% (high inhibition), using 100 μM of compound. A fourth group of 'very high' inhibition (>80%) is applicable only to isoenzyme hGSTA1-1, when using only 25 μM of compound (Table S5). The compounds with the strongest inhibition potency for hGSTP1-1 were further studied to determine their IC_{50} values from concentration–response curves (Figure 1, Table S6). Predictably, compounds with higher % inhibition potency exhibited lower IC_{50} values. It appears that the compounds are not, overall, as effective for hGSTP1-1 inhibition, as for hGSTA1-1 (Table 1). However, it is most interesting that some of them exhibited a clear preference with respect to a particular isoenzyme. For example, **6**, **8**, **9** and **15**, although weak inhibitors for the P1-1A allozyme at 100 μM (Table 1; \approx 41%, 0%, 0% and 24%, respectively), are rather potent for isoenzyme A1-1 at only 25 μM (\approx 86%, 88%, 59% and 96%, respectively). Even a more interesting behaviour is shown by certain compounds that demonstrated absolute selectivity for specific isoenzymes and/or allozymes. For example, **6** and **7**, the 5-mono- and 5,5'-di-phenyl-substituted benzophenones, show absolute selectivity for A1-1 over the P1-1B allozyme (Table 1; \approx 86% and 34% versus 0%, respectively), whereas additional absolute selectivity for A1-1 is shown by **7** over the P1-1C allozyme. In practice, **6** is also selective for A1-1 over the P1-1B allozyme (\approx 86% versus 3.0%, respectively). Likewise, **8** and **9**, the 5-mono- and 5,5'-di-brominated benzophenones, show absolute selectivity for A1-1 over P1-1A (Table 1; \approx 88% and 59% versus 0%, respectively), whereas additional absolute selectivity for A1-1 is shown by **8** over the P1-1B allozyme

and by **9** over the P1-1C allozyme. Even **15** can practically be regarded as one of absolute selectivity with hGSTA1-1 (\approx 96% inhibition) over hGSTP1-1C (14% inhibition), as the latter is diminished at 25 μM . On the other hand, **11**, **12** and **13** show numerically comparable inhibitory potencies with A1-1 and P1-1 (Table 1; **11**: 52% versus 31%; **12**: 68% versus 67%; **13**: 87% versus 62%), thus being adequate inhibitors for both isoenzymes, nevertheless still more potent with hGSTA1-1. On the basis of these observations, we went on to investigate further the modality of interaction between the most potent inhibitors and the target hGSTP1 allozymes by means of inhibition kinetics and *in silico* molecular modelling and docking. Moreover, to have a better understanding of the behaviour of these compounds with isoenzymes A1 and P1, we brought into context an *in silico* comparative approach for the proteins under study.

Kinetics of hGSTP1-1 inhibition by selected inhibitors

From the most potent inhibitors, we selected for enzyme inhibition kinetics those structures exhibiting distinctive chemical differences: a ketoxime (**11**), an aromatic N-acyl hydrazone (**13**) and an aliphatic N-acyl hydrazone (**15**). When using CDNB as a variable substrate, all compounds displayed purely competitive inhibition kinetics on the basis of the linearity observed for both the double-reciprocal Lineweaver–Burk graphs (Figures 2A and S3a,b) and their respective secondary derivatives (Figures 2B and S3d,e) (26,27), at various steady inhibitor concentrations. This behaviour suggests that each of the inhibitors competes with CDNB for the same binding site of the respective allozyme: calculated inhibition constants $K_{i(13/A)} = 63.6 \pm 3.0 \mu\text{M}$ (from Figure S3d), $K_{i(15/B)} = 198.6 \pm 14.3 \mu\text{M}$ (from Figure S3e) and $K_{i(11/C)} = 16.5 \pm 2.7 \mu\text{M}$ (from Figure 2B). Predictably, with GSH as a variable substrate, a mixed inhibition kinetics was observed, manifested by the lines of the double-reciprocal Lineweaver–Burk graph of initial velocities versus $[\text{GSH}]$, at various steady inhibitor concentrations (i.e. compound **11**), intersecting left of the reciprocal velocity axis (Figure S4a) (26,27). Furthermore, the linear correlation of the respective secondary derivative, depicting slope versus $[\text{inhibitor}]$ (Figure S4b), is supportive of a purely mixed type of inhibition (26,27). This equilibrium model predicts that the inhibitor binds to both the free enzyme and the enzyme–GSH complex, without product formation (26,27), interacting at a site other than the GSH-binding site, that being partly the catalytic CDNB-binding site, as shown earlier (Figure 2A,B). Interestingly, the same kinetic modality (e.g. purely competitive) had been observed earlier with **13** and hGSTA1-1, displaying, nonetheless, a substantially higher inhibitory potency (\approx 167-fold), $K_{i(13)} = 0.38 \pm 0.05 \mu\text{M}$ (7) as compared to $63.6 \pm 3.0 \mu\text{M}$ with hGSTP1-1. On the other hand, the potency of compound **15**, which was shown earlier to have a different inhibition modality with hGSTA1-1 (mixed hyperbolic) (7), is \approx 113-fold higher with hGSTA1-1, com-

Table 1: Some properties of 2,2'-dihydroxybenzophenones and their carbonyl N-analogues. **5-9**, ketones; **10-12**, ketoximes; **13-15**, N-acyl hydrazones. hGSTP1A, Ile104/Ala113; hGSTP1B, Val104/Ala113; hGSTP1C, Val104/Val113

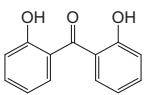
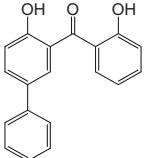
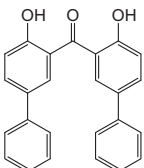
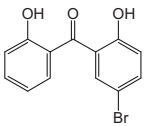
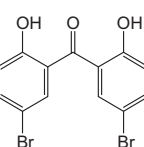
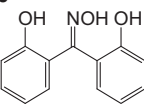
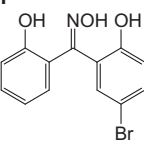
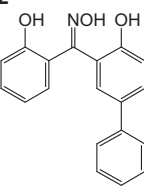
Compound no and structure	Molecular formula	Molecular weight	hGSTP1A inhibition (%) ^a	hGSTP1B inhibition (%) ^a	hGSTP1C inhibition (%) ^a	hGSTA1-1 inhibition (%) ^b
5 	C ₁₃ H ₁₀ O ₃	214	26.8 ± 3.4	12.4 ± 2.3	25.0 ± 4.6	–
6 	C ₁₉ H ₁₄ O ₃	290	41.3 ± 0.7	–	3.0 ± 4.7	86.1
7 	C ₂₅ H ₁₈ O ₃	366	1.5 ± 4.0	–	–	33.9
8 	C ₁₃ H ₉ BrO ₃	293	–	–	19 ± 3.5	87.7
9 	C ₁₃ H ₈ Br ₂ O ₃	372	–	11.0 ± 1.9	–	58.6
10 	C ₁₃ H ₁₁ N O ₃	229	17.0 ± 3.3	–	21.4 ± 0.8	40.5
11 	C ₁₃ H ₁₀ BrNO ₃	308	31.0 ± 4.7	23.0 ± 5.0	50.7 ± 5.0	52.3
12 	C ₁₉ H ₁₅ NO ₃	305	67.0 ± 4.6	37.7 ± 1.9	70.1 ± 1.3	67.7

Table 1: continued

Compound no and structure	Molecular formula	Molecular weight	hGSTP1A inhibition (%) ^a	hGSTP1B inhibition (%) ^a	hGSTP1C inhibition (%) ^a	hGSTA1-1 inhibition (%) ^b
13 	C ₂₀ H ₁₆ N ₂ O ₃	332	61.7 ± 4.2	30.7 0 ± 0.2	29.6 ± 1.7	87.4
14 	C ₁₉ H ₁₆ N ₃ O ₃	334	17 ± 2.2	21.8 ± 1.6	18.0 ± 0.7	31.8
15 	C ₁₅ H ₁₃ BrN ₂ O ₃	349	24.2 ± 4.8	40.7 ± 0.2	14.0 ± 5.0	96.1

^aThe errors shown were based on three assays.

^bData taken from reference 7 (mean values of three assays; 25 μM compound, error ≤5%).

(-) No enzyme inhibition was observed.

pared with hGSTP1-1, $K_{i(15)}$ 1.75 (7) versus 198.6 μM, respectively. Regardless of the different inhibition modality observed, both **13** and **15** are significantly weaker with the P1-1 isoenzyme, compared to A1-1. Taking into consideration the earlier discussion on the inhibition potency and the findings from the kinetics study, one can conclude that the compounds are directed to the H-site of the enzyme but with a varying selectivity for the particular isoenzyme, A1-1 and P1-1. Molecular modelling, docking and structural comparison studies may clarify certain aspects of this behaviour.

Molecular modelling and docking: in silico study of the selected inhibitors with hGSTA1-1 and hGSTP1-1 allozymes

Three allelic variants of hGSTP1-1 (variant A PDB code 11GS, variant B PDB code 1PGT), containing an Ile104-Val or Ala113Val substitution or a combination of both, have been studied for *in silico* binding together with hGSTA1-1 (PDB code 1GSE) and showed different interaction parameters.

In regard to the differences between hGSTA1-1 and hGSTP1-1, it is apparent that the binding site of the former is much wider due to the shift of the C-terminal eleven amino acid residues (res 210–221 in hGSTA1 forming an α-helix, whereas res 201–207 in hGSTP1-1 forming a closed loop) (Figure 3). Although the binding site of hGSTP1-1 remains essentially the same from three sides, on the fourth (upper) side, the flexible C-terminal structure in hGSTP1-1 diminishes the binding site volume. Hence, compounds bound in hGSTP1-1 have to occupy a more restricted site, reducing possible modes of binding and affecting interactions (Figures 4 and S5). This is in agreement with the findings from the screening experiments (Table 1) and the earlier discussion (cf. % inhibition with hGSTA1-1 versus hGSTP1-1).

As to the hGSTP1-1 allozymes, the *in silico* binding results show that the mutation between the allozymes A, B and C of the amino acid side chain at residue position 104 is ligand dependent. Indeed, in accord with the available crystal structures of hGSTP1*A, hGSTP1*B and hGSTP1*C (28,29), position 104 is localized in the H-site

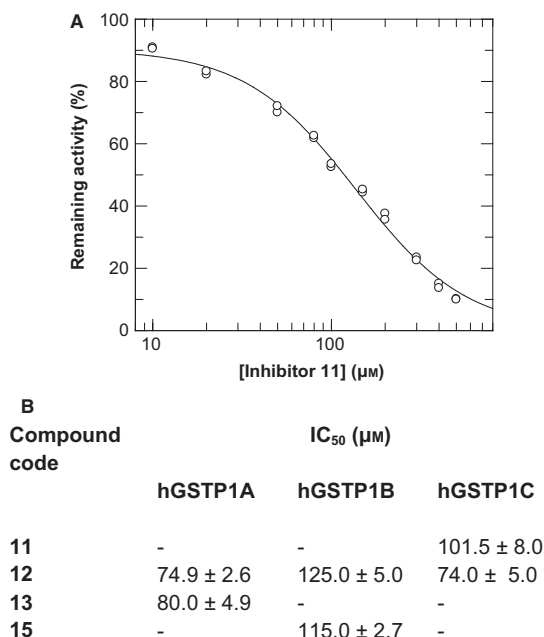


Figure 1: (A) Concentration–response graph for the determination of the IC₅₀ value for inhibitor **11** with hGSTP1-1C. The ‘concentration’ values (μM) are presented on logarithmic scale, whereas the ‘response’ values (as % ratios of inhibited over uninhibited rates) are presented on the ‘Remaining activity’ axis. The graph was produced using GraFit3. The IC₅₀ values determined from such graphs for inhibitors **11**, **12**, **13** and **15** are given in (B).

of hGSTP1-1 and can affect enzyme activity in several ways dependent on the ligand (30). The Ile104Val mutation affects the shape of the active site (Figure 4B) because Val104 occupies a smaller volume than Ile104, allowing the accommodation of larger ligands (28). Also, residue 104 is close to the functional residue Tyr108, important in the catalytic mechanism of hGSTP1-1 by stabilizing the intermediate complex (31,32). In addition, mutation Ile104-Val has shown to alter the hydrophobicity/hydrophilicity status of the H-site of hGSTP1-1 by influencing the number of active-site water molecules that can interact during substrate binding and/or product release (32,33). These factors explain, in part at least, the selectivity of the compounds between hGSTA1-1 and hGSTP1-1 isoenzymes as well as between the hGSTP1-1 allozymes. Benzophenone analogues containing a hydrophobic moiety (e.g. phenyl ring) at position 5 are shown to optimally bind differently in hGSTA1-1 (Figure 4B, ligands in blue) and in hGSTP1-1 (Figure 4B, ligands in green for allozyme A and in red for allozymes B and C), the former isoenzyme not exposing the hydrophobic group to solvent, while the latter with a more open binding site having larger exposure to solvent. There are also differences in binding between hGSTP1-1 allozymes A and B,C, with A having ligands bound deeper in the pocket (Figure S6, green ligands) with reduced exposure of the ligand’s hydrophobic groups, compared to B and C (Figure S6, red ligands). This is in agreement with the observation that all aryl-substituted

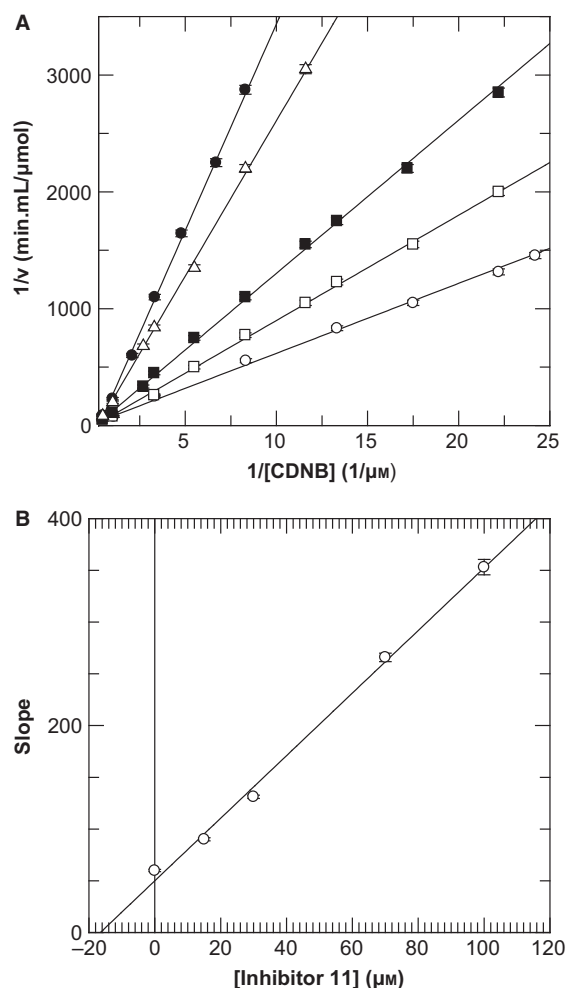


Figure 2: Purely competitive inhibition kinetics of allozyme hGSTP1-1C with inhibitor **11** using CDNB as a variable substrate. (A) Lineweaver–Burk graph of initial velocities versus [CDNB] at different concentrations of **11** (○ 0, □ 15, ■ 30, △ 70 and ● 100 μM). (B) Secondary graph for inhibitor **11** derived from data of primary graph (A). The inhibition constant K_i is the intercept on the basis axis of the secondary graph (B). Points are average of three enzyme assays. The graphs were produced using GraFit3.

compounds (6,12,13) show a stronger inhibition with hGSTP1-1A than the hGSTP1-1B,C allozymes (Table 1). However, the diaryl-substituted **7** fails to bind effectively to any of the three hGSTP1-1 allozymes, due to the size and character (hydrophobic) of the substituting groups in the restricted polar binding site volume. Interestingly, the derivatization of the benzophenone carbonyl group (ketoximes **10–12**, Figure S7a) and N-acyl hydrazones (**13–15**, Figure S7b) enhances the inhibition potency towards the allozymes (Table 1), possibly due to the formation of at least one hydrogen bond and reorientation of the compound in the binding pocket. This behaviour probably indicates an alternative (flipped) orientation in the enzyme-binding site. Furthermore, from the *in silico* study, it is apparent that the mode of binding to the P1-1 allozymes changes when compounds become amphipathic with the introduction of a

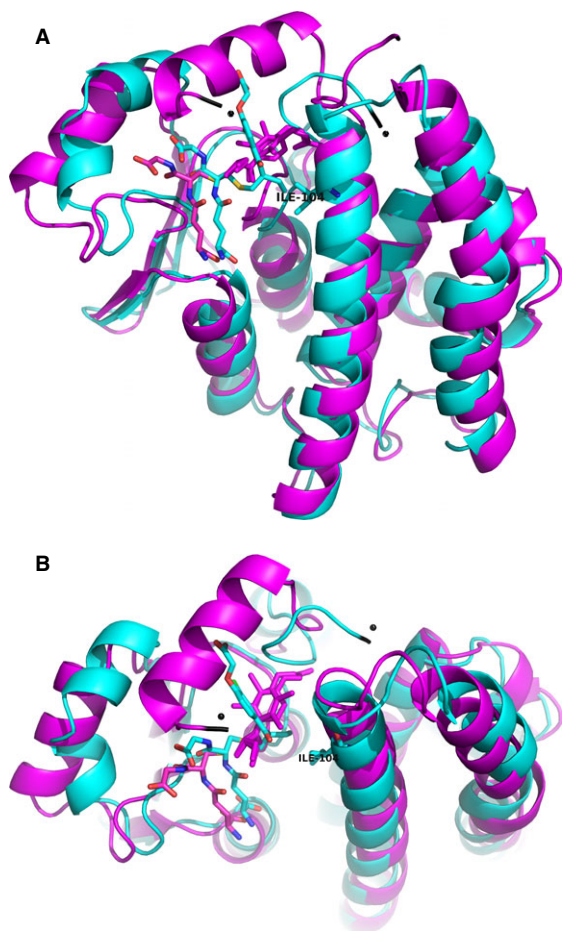


Figure 3: Orthogonal views of the structural superposition between hGSTA1-1 (magenta) and hGSTP1-1 (cyan). The C-terminals of both proteins are colored black and marked by a dot. Bound ligands (GSH and inhibitors) are depicted in stick representation, the S atom in yellow, N atoms in blue and O atoms in red. The figure was produced using PYMOL v.1.5.

bromine atom at position 5 (**6** versus **8**, Figure S8a; **11** versus **12**, Figure S8b) but not at both positions 5 and 5' (**7** and **9**). This is in line with the observed differences in inhibition potency against the hGSTP1-1 allozymes (Table 1).

Conclusion

(i) There is no uniform binding mode of the compounds in hGSTA1-1- and hGSTP1-1-binding sites but rather specific modes related to their substitution (i.e. phenyl or bromine groups) or carbonyl-derivatization pattern; (ii) disubstituted benzophenones (at positions 5 and 5') lose almost entirely their inhibition potency towards hGSTP1-1, compared to a fairly strong inhibitory potency towards hGSTA1-1, thus displaying isoenzyme specificity (A1-1 versus P1-1); (iii) monosubstituted benzophenones (at position 5) lose entirely their inhibition potency towards certain hGSTP1-1 allozymes and retain it towards others, thus displaying remarkable absolute allozyme specificity

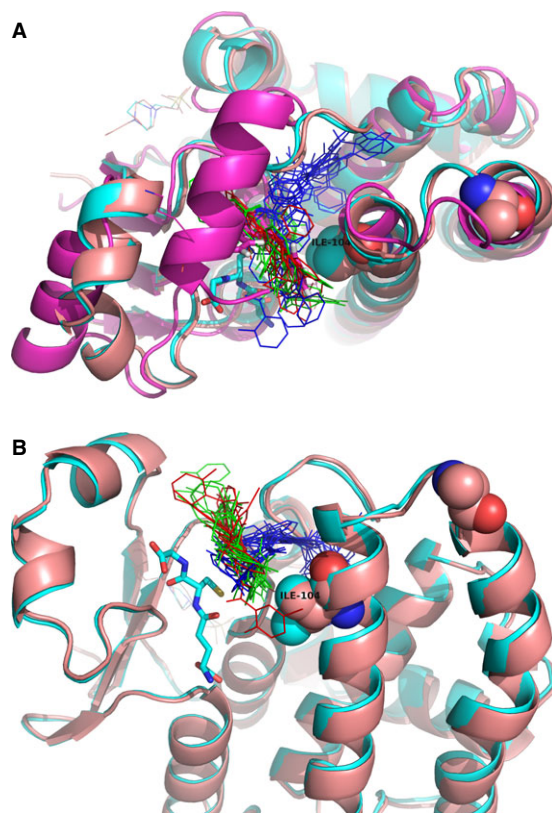


Figure 4: (A) Clustering of compound **6** optimal binding positions on hGSTA1-1 (magenta with blue ligands), hGSTP1-1 allozyme A (cyan with green ligands) and allozymes B and C (pink with red ligands) as predicted by *in silico* molecular docking. It is evident that clustering occurs around the position of Ile/Val104 present in the binding site of P1-1, with the A1-1 being wider. (B) Structural superposition between hGSTP1-1 allozyme A (cyan with green ligands) and hGSTP1-1 allozyme B (pink with red ligands) with clustering of compound **8** optimal binding positions, as predicted by *in silico* molecular docking. Also present are optimal binding positions of **8** on hGSTPA1-1 (blue ligands). It is evident that binding positions taken by **8** in A1-1 (where **8** is a potent inhibitor) cannot be taken in P1-1A,B due to the restricted volume. Predicted positions for **8** in P1-1A,B (green and red, respectively) cannot justify inhibitory phenomena for the two allozymes (cf. % inhibition in Table 1). The variant amino acid residues are shown as space filling models. All ligands are depicted in line representation. The cosubstrate GSH is depicted in stick representation, the S atom in yellow, N atoms in blue and O atoms in red. The figure is created using PYMOL v.1.5.

(P1-1A versus P1-1B versus P1-1C); and (iv) the derivatization on the carbonyl carbon for obtaining ketoximes and N-acyl hydrazones enhances their inhibition potency towards hGSTP1-1.

Acknowledgments

This work was partly supported by the action THALES: 'Glutathione transferases, multifunctional molecular tools in red and green biotechnology' falling under the Operational

Programme 'Education and Lifelong Learning' and is cofinanced by the European Social Fund and National Resources.

References

- Acuna U.M., Jancovski N., Kenelly E.J. (2013) Polyisoprenylated benzophenones from Clusiaceae: potential drugs and lead compounds. *Curr Top Med Chem*;9:1560–1580.
- Alvarez C., Alvarez R., Corchete P., Pérez-Melero C., Peláez R., Medarde M. (2008) Naphthylphenstatins as tubulin ligands: synthesis and biological evaluation. *Bioorg Med Chem*;16:8999–9008, and references cited therein.
- Odrawaz-Sypniewski M.R., Tsoungas P.G., Varvounis G., Cordopatis P. (2009) Xanthone in synthesis: a reactivity profile via directed lithiation of its dimethyl ketal. *Tetrahedron Lett*;50:5981–5983.
- Gardikis Y., Tsoungas P.G., Potamitis C., Zervou M., Cordopatis P. (2011) Xanthenes in heterocyclic synthesis. An efficient route for the synthesis of C-3 o-hydroxyaryl-substituted 1,2-benzisoxazoles and their N-oxides, potential scaffolds for angiotensin (II) antagonist hybrid peptides. *Heterocycles*;83:1077–1091.
- Gardikis Y., Tsoungas P.G., Potamitis C., Zervou M., Pairs G., Cordopatis P. (2011) Xanthenes in heterocyclic synthesis. An efficient and general route for the synthesis of regioselectively substituted phthalazines. *Heterocycles*;83:1291–1302.
- Zoi O.G., Thireou T.N., Rinotas V.E., Tsoungas P.G., Eliopoulos E.E., Douni E.K., Labrou N.E., Clonis Y.D. (2013) Designer xanthone: an inhibitor scaffold for MDR-involved human glutathione transferase isoenzyme A1-1. *J Biomol Screen*;18:1092–1102.
- Perperopoulou F.D., Tsoungas P.G., Thireou T.N., Rinotas V.E., Douni E.K., Eliopoulos E.E., Labrou N.E., Clonis Y.D. (2014) 2,2'-Dihydroxybenzophenones and their carbonyl N-analogues as inhibitor scaffolds for MDR-involved human glutathione transferase isoenzyme A1-1. *Bioorg Med Chem*;22:3957–3970.
- Frova C. (2006) Glutathione transferases in the genomics era: New insights and perspectives. *Biomol Eng*;23:149–169.
- Kodera Y., Isobe K., Yamauchi M., Kondo K., Akiyama S., Ito K., Nakashima I., Takagi H. (1994) Expression of glutathione-S-transferases alpha and pi in gastric cancer: a correlation with cisplatin resistance. *Cancer Chemother Pharmacol*;34:203–208.
- Pandya U., Srivastava S.K., Singhal S.S., Pal A., Awasthi S., Zimniak P., Awasthi Y.C., Singh S.V. (2000) Activity of allelic variants of Pi class human glutathione S-transferase toward chlorambucil. *Biochem Biophys Res Commun*;278:258–262.
- Ishimoto T.M., Ali-Osman F. (2002) Allelic variants of the human glutathione S-transferase P1 gene confer differential cytoprotection against anticancer agents in *Escherichia coli*. *Pharmacogenetics*;12:543–553.
- Ekhart C., Doodeman V.D., Rodenhuis S., Smits P.H., Beijnen J.H., Huitema A.D. (2009) Polymorphisms of drug-metabolizing enzymes (GST, CYP2B6 and CYP3A) affect the pharmacokinetics of thiotepa and tepla. *Br J Clin Pharmacol*;67:50–60.
- Sau A., Trengo F.P., Valentino F., Federici G., Caccuri A.M. (2010) Glutathione transferases and development of new principles to overcome drug resistance. *Arch Biochem Biophys*;500:116–122.
- Johansson K., Ito M., Schopuizen C.M.S., Then-gumtharayil S.M., Heuse V.D., Zhang J., Shimoji M., Vahter M., Ang W.H., Dyson P.J., Shibata A., Shuto S., Ito Y., Abe H., Morgenstern R. (2011) Characterization of new potential anticancer drugs designed to overcome glutathione transferase mediated resistance. *Mol Pharmaceutics*;8:1698–1708.
- Razza A., Galili N., Smith S., Godwin J., Lancel J., Melchert M., Jones M., Keck J.G., Meng L., Brown G.L., List A. (2009) Phase 1 multicenter dose-escalation study of ezatiostat hydrochloride (TLK199 tablets), a novel glutathione analog prodrug, in patients with myelodysplastic syndrome. *Blood*;113:6533–6540.
- Morgan A.S., Ciaccio P.J., Tew K.D., Kauvar L.M. (1996) Isozyme-specific glutathione S-transferase inhibitors potentiate drug sensitivity in cultured human tumor cell lines. *Cancer Chemother Pharmacol*;37:363–370.
- Ali-Osman F., Akande O., Antoun G., Mao J.X., Buolamwini J. (1997) Molecular cloning, characterization, and expression in *Escherichia coli* of full-length cDNAs of three human glutathione S-transferase Pi gene variants. Evidence for differential catalytic activity of the encoded proteins. *J Biol Chem*;272:10004–10012.
- Paumi C.M., Smitherman P.K., Townsend A.J., Morrow C.S. (2004) Glutathione S-transferases (GSTs) inhibit transcriptional activation by the peroxisomal proliferator-activated receptor gamma (PPAR gamma) ligand, 15-deoxy-delta 12,14-prostaglandin J2 (15-d-PGJ2). *Biochemistry*;43:2345–2352.
- Sastry G.M., Adzhigirey M., Day T., Annabhimoju R., Sherman W. (2013) Protein and ligand preparation: parameters, protocols, and influence on virtual screening enrichments. *J Comput Aid Mol Des*;27:221–234.
- Bowers K.J., Chow E., Xu H., Ron D.O., Michael E.P., Brent G.A., John K.L., Kolossváry I., Mark M.A., Federico S.D., John S.K., Shan Y., David S.E. (2006) "Algorithms Scalable for Simulations Molecular Dynamics on Clusters Commodity," Proceedings of the ACM/Conference IEEE on Supercomputing (SC06), Tampa Florida, November 11–17, 2006.
- Hawkins P.C., Skillman A.G., Warren G.L., Ellingson B.A., Stahl M.T. (2010) Conformer generation with OMEGA: algorithm and validation using high quality structures from the Protein Databank and Cambridge Structural Database. *J Chem Inf Model*;50:572–584.
- Hawkins P.C.D., Skillman A.G., Nicholls A. (2007) Comparison of shape-matching and docking as virtual screening tools. *J Med Chem*;50:74–82.
- Friesner R.A., Banks J.L., Murphy R.B., Halgren T.A., Klicic J.J., Mainz D.T., Repasky M.P., Knoll E.H., Shaw

- D.E., Shelley M., Perry J.K., Francis P., Shenkin P.S. (2004) Glide: a new approach for rapid, accurate docking and scoring. 1. Method and assessment of docking accuracy. *J Med Chem*;47:1739–1749.
24. Halgren T.A., Murphy R.B., Friesner R.A., Beard H.S., Frye L.L., Pollard W.T., Banks J.L. (2004) Glide: a new approach for rapid, accurate docking and scoring. 2. Enrichment factors in database screening. *J Med Chem*;47:1750–1759.
25. Copeland R.A. (2003) Mechanistic considerations in high-throughput screening. *Anal Biochem*;320:1–12.
26. Dixon M., Webb E. (1997) *Enzymes*, 3rd edn. London, UK: Longman Group Ltd; 332–381 p.
27. Leskovac V. (2003) *Comprehensive Enzyme Kinetics*. New York: Kluwer Academic Publishers; 73–94, 95–110, 139–170 p.
28. Ji X.H., Blaszczyk J., Xiao B., O'Donnell R., Hu X., Herzog C., Singh S.V., Zimniak P. (1999) Structure and function of residue 104 and water molecules in the xenobiotic substrate-binding site in human glutathione S-transferase P1-1. *Biochemistry*;38:10231–10238.
29. Parker L.J., Ciccone S., Italiano L.C., Primavera A., Oakley A.J., Morton C.J., Hancock N.C., Lo Bello M., Parker M.W. (2008) The anti-cancer drug chlorambucil as a substrate for the human polymorphic enzyme glutathione transferase P1-1: kinetic properties and crystallographic characterisation of allelic variants. *J Mol Biol*;380:131–144.
30. Dragovic S., Venkataraman H., Begheijn S., Vermeulen N.P., Commandeur J.N. (2014) Effect of human glutathione S-transferase hGSTP1-1 polymorphism on the detoxification of reactive metabolites of clozapine, diclofenac and acetaminophen. *Toxicol Lett*;224:272–281.
31. Oakley A.J., LoBello M., Battistoni A., Ricci G., Rossjohn J., Villar H.O., Parker M.W. (1997) The structures of human glutathione transferase P1-1 in complex with glutathione and various inhibitors at high resolution. *J Mol Biol*;274:84–100.
32. Zimniak P., Nanduri B., Pikuła S., Bandorowicz-Pikuła J., Singhal S.S., Srivastava S.K., Awasthi S., Awasthi Y.C. (1994) Naturally occurring human glutathione S-transferase GSTP1-1 isoforms with isoleucine and valine in position 104 differ in enzymic properties. *Eur J Biochem*;224:893–900.
33. Hu X., Xia H., Srivastava S.K., Herzog C., Awasthi Y.C., Ji X.H., Zimniak P., Singh S.V. (1997) Activity of four allelic forms of glutathione S-transferase hGSTP1-1 for diol epoxides of polycyclic aromatic hydrocarbons. *Biochem Biophys Res Commun*;238:397–402.

Supporting Information

Additional Supporting Information may be found in the online version of this article:

Appendix S1. Expression and purification of hGSTP1-1 allozymes A, B and C.

Table S1. Glide Receptor grid, Ligand Docking, restrain and postoptimization output parameters.

Table S2. Scoring results of optimal binding positions for compounds 5-15 on hGSTA1-1, and hGSTP1-1 allozymes A and B using the OPLS-05 force field.

Table S3. Desmond 3.6 Model System and Molecular Dynamics Simulation parameters.

Table S4. Summary of purification results for hGSTP1-1 allozymes A, B and C.

Table S5. Grouping of compounds 5-15 according to their inhibition potency against human hGST isoenzymes A1-1 and P1-1.

Table S6. Determined IC₅₀ values for the stronger inhibitors against hGSTP1-1 allozymes A, B and C.

Figure S1. Molecular dynamics on the hGSTP1-1 allozyme B. The results of a 12 ns run on Desmond 3.6 are displayed every 50 frames (0.24 ns) in different colours using PyMOL. Only the backbone is shown in cartoon mode with the Ile104 side chain shown in line mode to indicate the rotamers.

Figure S2. Histogram presenting the relative inhibitory potency of the compounds tested against hGST isoenzymes P1-1 and A1-1.

Figure S3. Purely competitive inhibition kinetics of hGSTP1-1 with inhibitors 13, 15 and 11 using CDNB as a variable substrate.

Figure S4. Mixed inhibition kinetics of hGSTP1-1 with inhibitor 11 using GSH as a variable substrate.

Figure S5. Structural superposition between hGSTA1-1, and hGSTP1-1 allozymes A and B with clustering of compound 12 optimal binding positions.

Figure S6. Structural superposition between hGSTP1-1 allozyme A and allozymes B,C with clustering of compound 6 optimal binding positions.

Figure S7. Optimal binding positions for ketoximes (10, 11, 12) and N-acyl hydrazones (13, 14, 15) on the hGSTP1-1 allozyme A.

Figure S8. Optimal binding positions for 2,2'-dihydroxybenzophenones 6 and 8, and for the respective ketoximes 11 and 12 on hGSTP1-1 allozyme A.